Earthquakes and Structures, *Vol. 10, No. 1 (2016) 211-238*
DOI: http://dx.doi.org/10.12989/eas.2016.10.1.211

Combination rules and critical seismic response of steel buildings modeled as complex MDOF systems

Alfredo Reyes-Salazar[*1], Federico Valenzuela-Beltran[1], David de Leon-Escobedo[2], Eden Bojorquez-Mora[1] and Arturo López Barraza[1]

[1]Facultad de Ingeniería, Universidad Autónoma de Sinaloa, Ciudad Universitaria, Culiacán Sinaloa, México
[2]Facultad de Ingeniería, Universidad Autónoma del Estado de México, Ciudad Universitaria, Toluca, Estado de México, México

(Received December 27, 2013, Revised March 1, 2015, Accepted October 26, 2015)

Abstract. The Maximum seismic responses of steel buildings with perimeter moment resisting frames (MRF), modeled as complex MDOF systems, are estimated for several incidence angles of the horizontal components and the critical one is identified. The accuracy of the existing rules to combine the effects of the individual components is also studied. Two and three components are considered. The critical response does not occur for principal components and the corresponding incidence angle varies from one earthquake to another. The critical response can be estimated as 1.40 and 1.10 times that of the principal components, for axial load and interstory shears, respectively. The rules underestimate the axial load but reasonably overestimate the shears. The rules are not always inaccurate in the estimation of the combined response for correlated components. On the other hand, totally uncorrelated (principal) components are not always related to an accurate estimation. The correlation of the individual effects (ρ) may be significant, even for principal components. The rules are not always associated to an inaccurate estimation for large values of ρ, and small values of ρ are not always related to an accurate estimation. Only for perfectly uncorrelated harmonic excitations and elastic analysis of SDOF systems, the individual effects of the components are uncorrelated and the rules accurately estimate the combined response. The degree of correlation of the components, the type of structural system, the response parameter under consideration, the location of the structural member and the level of structural deformation must be considered while estimating the level of underestimation or overestimation.

Keywords: critical response; steel buildings; seismic design codes; combination rules; effect of individual components; correlation of effects; MDOF and SDOF systems

1. Introduction

Seismic analysis and design procedures have been significantly modified around the world after the occurrence of catastrophic earthquakes. Several methods have been suggested in many codes including the equivalent lateral force procedure and several types of dynamic analysis procedures. Our understanding of the earthquake phenomenon has improved significantly during the last years.

∗Corresponding author, Professor, E-mail: reyes@uas.edu.mx

http://www.techno-press.com/journals/eas&subpage=7 ISSN: 2092-7614 (Print), 2092-7622 (Online)

This improved understanding needs to be studied in the context of the estimation of structural responses since they are the primary interests of structural engineers. Due to the progress in the computer technology, the computational capabilities have significantly increased in the recent years. It is now possible to estimate the seismic response behavior by modeling structures in three dimensions and applying the seismic loadings in time domain as realistically as possible. Responses obtained in this way represent the *best estimate* and the accuracy of other simplified methods can then be judged by comparing the responses obtained by them with those of the *best estimate*. These comparisons are essential to improve our understandings and to design more seismic-load tolerant structures even by using simplified design procedures routinely used in the profession.

Energy released during an earthquake travels in the form of waves. They are measured in the form of two horizontal and one vertical translational acceleration time histories. Rotational excitations are not measured and are completely ignored in the analysis. In addition, for far-source ground motions, the effect of the vertical component is usually smaller than those of the horizontal components and is consequently neglected. Additional bases to neglect the vertical component effect are that building designs allow for gravity loads, which provides for a high factor of safety in the vertical direction (Newmark and Hall 1982, Salmon *et al.* 2009). Thus, when a structure is analyzed, two horizontal recorded components are generally applied along their two major axes. The major implication of this practice if that the orientation of the critical response is commonly ignored in the analysis.

In routine simplified analyses, structural responses are estimated by applying each component one at a time and then their effects are combined in many different ways. The commonly used procedures are the 30 percent (*30%*) and the Square Root of Summation Squares (*SRSS*) combination rules. Many codes around the world like International Building Code (IBC, 2009) and The México City Code (RCDF 2004) consider these combination rules. The codes, however, do not explicitly state the applicability of these rules. It is not specified how to select the critical orientation of the orthogonal components nor the type of structures (simple or complex systems) to be considered or if the rules can be applied to both, elastic and inelastic behavior. It is not specified either if the individual responses produced by each component should be collinear (axial load in columns) or non-collinear (interstory shears), or if the rules should be applied to single or simultaneously to multiple response parameters.

Some of the abovementioned issues are explicitly addressed in this paper. The orientation of the seismic components that produce the critical response is investigated. The accuracy of these combination rules, essentially developed for linear modal analysis procedures is studied. The rules implicitly assume that the components and their corresponding effects are uncorrelated. The effect of the correlation of the components, and that of the individual effects in the accuracy of the rules, is also studied.

2. Literature review and objectives

The ways of combining the individual effects of the seismic components as well as their critical orientation have been a topic of interest to the civil engineering profession. Penzien and Watabe (1975) stated that the three components of an earthquake are uncorrelated (denoted hereafter as principal components) along a set of axes generally denoted as principal axes. The major principal axis is horizontal and directed toward the epicenter, the intermediate axis is horizontal and perpendicular to the orientation of the major component, and the minor principal axis is vertical. The critical response could be obtained when these principal components are applied. Rosenblueth (1980) stated "lack of correlation of the principal accelerograms insures that responses are also uncorrelated". Smeby and Der Kiureghian (1985) observed that, for response spectra analysis of linear structures, when the two horizontal principal components are not along the structural principal axes, the effect of correlation is small and that if the two horizontal components have identical or nearly identical intensities, then the effect of correlation disappears. Newmark (1975) and Rosenblueth and Contreras (1977) proposed the *Percentage Rule* to approximate the combined response as the sum of the 100% of the response resulting from one component and some percentage (λ) of the responses resulting from the other two components. To combine the two horizontal components, Newmark (1975) suggested λ to be 40% and Rosenblueth and Contreras (1977) suggested λ to be 30%.

Many other studies, regarding the combination of the seismic responses produced by two or three components, have been reported. Using elastic analysis and a simple three-dimensional structure, Wilson *et al.* (1995) observed that the percent combination rule could underestimate the design forces in some members. Lopez *et al.* (2000) proposed a formula to calculate the critical value of structural responses due to the principal horizontal components acting along any incidence angle with respect to the structural axes. Menun and Der Kiureghian (2000) developed a response-spectra-based procedure to predict the envelope that bounds the simultaneous action of two or more seismic response parameters for linear structures. For modal analysis, Der Kiureghian (1981) and Wilson *et al.* (1981) proposed the *Complete Quadratic Combination* (*CQC*) rule to combine modal responses due to a single seismic component. Smeby and Der Kiureghan (1985), Lopez and Torres (1996) and Lopez *et al*. (2004) proposed an extension of the *CQC* rule, known as the *CQC*3 rule, to combine modal responses due to two and three seismic components. They verified the *CQC*3 rule by considering building-type structures with rectangular geometry and applied the rule to determine the critical response of elastic structures subjected to two and three seismic components with arbitrary spectra. Menun and Der Kiureghian (1998) extended these studies by considering more complex three-dimensional curved bridge structures subjected to two horizontal components. López *et al*. (2001) conducted a similar study to combine the two horizontal components with a range of one-story systems with symmetrical and unsymmetrical plan, and two multi-story buildings. Hernández and López (2003) extended the work of López *et al.* (2001) by considering the effect of the vertical component. The critical response was calculated for two cases: (i) assuming that a principal seismic component is along the vertical direction (*CQC*3 rule) and (ii) when a component does not coincide with the vertical direction (*GCQC*3 rule). They observed that if a principal component does not coincide with the vertical direction, the critical response would be underestimated using the *GCQC*3 rule. Lopez *et al*. (2006) investigated the response spectra characteristics of the principal components and determined the ratios between the spectra of the components. Beyer and Bommer (2007) studied several aspects involved when selecting and scaling records for bi-directional analysis post-processing the results of such analysis. They showed that the structural response varies depending on the angle of incidence of the ground motions with respect to the structural axes and that the median response for all possible angles could be the most appropriate quantity. Rigato and Medina (2007) examined the effect that the angle of incidence has on single-storey structure subjected to bi-directional ground motions. They demonstrated that applying bi-directional components along the principal axes of the structure could underestimate the inelastic peak demands.

More recently, Bisadi and Head (2010) investigated the orthogonal effects in nonlinear analysis of single-span bridges subjected to multi-component earthquake excitations. They showed that the critical excitation angle is not the same in linear and nonlinear models and that the American Association of State Highway and Transportation Officials (AASTHO) procedure to estimate the combined effects of separate unidirectional excitations may underestimate the maximum probable response. Mackie and Cronin (2011) studied the effect of the incidence angle for three-dimensional excitation in the response of highway bridges. They computed single-degree-of-freedom (SDOF) elastic and inelastic mean spectra by using various orientation techniques. They found that the incidence angle has a negligible effect on mean ensemble response. Bisadi and Head (2011) proposed to use of the 40% rule with the major component of earthquakes for nonlinear time history analysis of bridges. Grant (2011), developed a new program for matching the major and minor axis spectra of two horizontal ground-motion components simultaneously to two target spectra, using wavelets. It was shown that the program can effectively match the major and minor axis spectra of the record to two individual target spectra, where the two targets are representative of either expected major and minor axis demand or the mean demand. Tsourekas Athanatopoulou (2013), by using six reinforce concrete single-storey models, showed that the types of analysis suggested in the Nuclear Regulatory Guide produce smaller response values than the maximum ones over all incident angles.

In spite of the important contributions of the previous studies on combination rules, most of them were limited to elastic analysis applied to SDOF systems or simplified plane concrete frames with a few stories connected by rigid diaphragms. They did not consider the inelastic behavior of the structural elements existing in actual 3D structural systems and the appropriate energy dissipation mechanisms. Reyes-Salazar *et al.* (2000), Reyes-Salazar and Haldar (1999, 2000, 2001a, 2001b) and Bojorquez *et al.* (2010) found that strong-column weak-beam moment resisting steel frames are very efficient in dissipating earthquake-induced energy and that the dissipated energy has an important effect on the structural response. More recently, Reyes-Salazar *et al.* (2004, 2008), by using nonlinear time history analysis of complex multi-degree of freedom (MDOF) systems, observed that both the *30%* and the *SRSS* rules could underestimate the combined response and that the energy dissipation mechanisms should be considered as accurately as possible. However, realistic structural systems, the critical incidence angle and the effect of correlation of the earthquake components on the accuracy of the rules, were not considered in these studies. The critical incidence angle of the seismic components, the accuracy of combination rules, the effect of correlation of the components and the dissipation of energy in the structure, are re-examined considering more realistic and complex structural systems. A nonlinear response analysis technique is used by considering the responses given by a computer program specifically developed for this purpose.

The specific issues addressed in this study are: a) the critical orientation of the orthogonal seismic components for collinear and non-collinear response parameters considering several incidence angles of the components and structures modeled as complex MDOF systems; b) the accuracy of the commonly used combination rules for complex MDOF systems for elastic and inelastic behavior and for collinear en non-collinear response parameters and c) the accuracy of the rules for simplified systems and loading condition. To comprehensively study these issues, the seismic responses of some structural models are estimated as accurately as possible by using nonlinear three-dimensional time history analysis. The degree of correlation of the seismic components and their effects, for the normally recorded (denoted hereafter as normal components) and the uncorrelated (principal) components are considered. The responses of steel buildings with moment resisting steel frames (MRF) are specifically studied.

3. Methodology

3.1 Mathematical formulation

To satisfy the objectives of the study, the seismic responses of some steel building models are evaluated as accurately as possible using an efficient assumed stress-based finite element algorithm developed by the authors and their associates (Gao and Haldar 1995, Reyes-Salazar 1997). The procedure estimates nonlinear seismic responses in time domain considering material and geometry nonlinearities. In this approach, an explicit form of the tangent stiffness matrix is derived without any numerical integration. Fewer elements can be used in describing a large deformation configuration without sacrificing any accuracy and the material and geometric nonlinearities can be incorporated without losing its basic simplicity. It gives very accurate results and is very efficient compared to the commonly used displacement-based approach. The procedure and the algorithm, implemented in a computer program, have been extensively verified using available theoretical and experimental results (Reyes-Salazar and Haldar 2000, Reyes-Salazar and Haldar 2001b). The details of the theory of this approach are out of the scope of this study.

3.2 Structural models

3.2.1 Complex MDOF systems

Three consulting firms were commissioned to perform the design of several model buildings as part of the SAC steel project (FEMA, 2000). They were designed according to the code requirements for the following three cities: Los Angeles (UBC, 1994), Seattle (UBC, 1994) and Boston (BOCA, 1993). The 3- and 9- story buildings, representing Los Angeles area and the Pre-Northridge Designs, are considered in this study to address the issues raised earlier. They will be denoted hereafter as Models 1 and 2, respectively. The elevations, plans models showing the location of the perimeter MRF (indicated by continuous lines), and the particular structural members considered in the study, are shown in Fig. 1. The beam and columns sections of the models are given in Table 1. The columns of the perimeter MRF of Model 1 are considered to be fixed at the base while those of Model 2 are assumed to be pinned. In all these frames, the columns are assumed to be made of Grade-50 steel and the girders are of A36 steel. For both models, the gravity columns are considered to be pinned at the base. Near rigid struts were used to consider the slab effect. All the columns in the MRF bend about the strong axis. The strong axis of the gravity columns is oriented in the *N-S* direction. The designs of the MRF in the two orthogonal directions were practically the same. The damping in the models is considered to be 5% of the critical damping; the same damping is used in the codified approaches. The fundamental periods of Model 1 are estimated to be 1.03, 0.99 and 0.07 sec., for the *N-S* (horizontal), *E-W* (horizontal) and vertical directions, respectively. The corresponding values for Model 2 are 2.22, 2.11 and 0.16 sec. Additional information for the models can be obtained from the SAC steel project reports (FEMA, 2000).

In this study, the steel buildings are modeled as complex MDOF systems. Each column is represented by one element and each girder of the MRF is represented by two elements, having a node at the mid-span. Each node is considered to have six degrees of freedom. The total number of degrees of freedom is 846 and 3408, for Models 1 and 2, respectively.

3.2.2 Simplified systems.

It is stated in Sections 1 and 2 of the paper that most of the studies regarding the combination

Table 1 Beam and columns sections for the SAC models

MODEL	STORY	MOMENT RESISTING FRAMES			GRAVITY FRAMES		
		COLUMNS		GIRDERS	COLUMNS		BEAMS
		EXTERIOR	INTERIOR		BELOW PENTHOUSE	OTHERS	
1	1\2	W14×257	W14×311	W33×118	W33×118	W14×68	W18×35
	2\3	W14×257	W14×312	W30×116	W30×116	W14×68	W18×35
	3\Roof	W14×257	W14×313	W24×68	W24×68	W14×68	W16×26
2	-1/1	W14×370	W14×500	W36×160	W36×160	W14×193	W18×44
	1/2	W14×370	W14×500	W36×160	W36×160	W14×193	W18×35
	2/3	W14×370	W14×500,W14×455	W36×160	W36×160	W14×193,W14×145	W18×35
	3/4	W14×370	W14×455	W36×135	W36×135	W14×145	W18×35
	4/5	W14×370,W14×283	W14×455,W14×370	W36×135	W36×135	W14×145,W14×109	W18×35
	5/6	W14×283	W14×370	W36×135	W36×135	W14×109	W18×35
	6/7	W14×283,W14×257	W14×370,W14×283	W36×135	W36×135	W14×109,W14×82	W18×35
	7/8	W14×257	W14×283	W30×99	W30×99	W14×82	W18×35
	8/9	W14×257,W14×233	W14×283,W14×257	W27×84	W27×84	W14×82,W14×48	W18×35
	9/Roof	W14×233	W14×257	W24×68	W24×68	W14x×8	W16×26

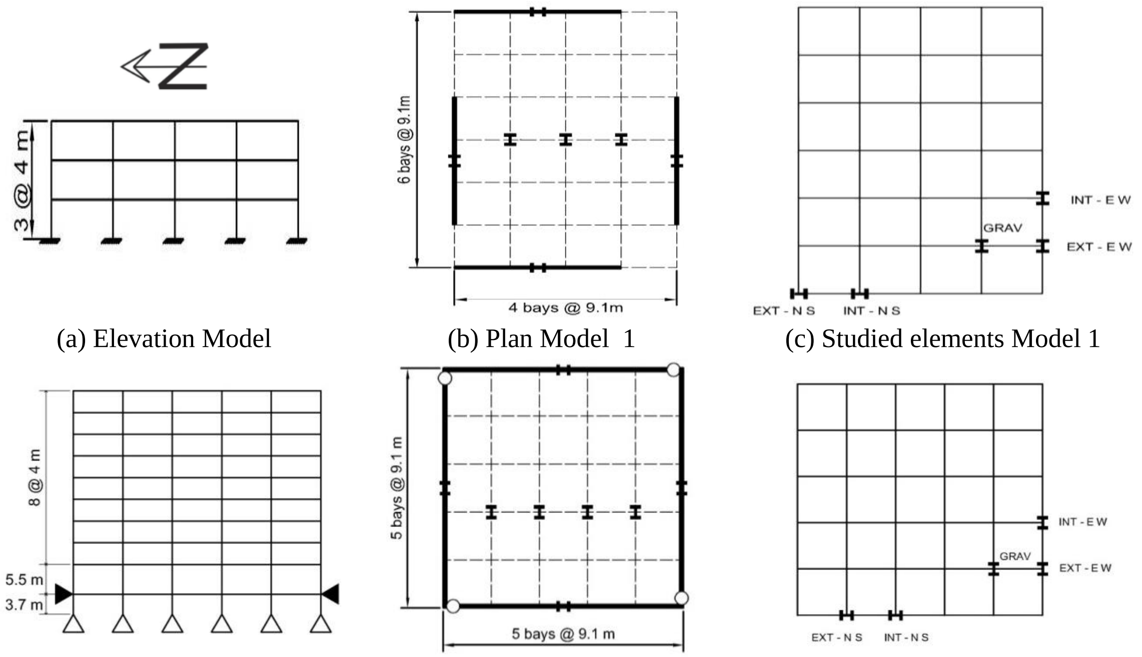

(a) Elevation Model (b) Plan Model 1 (c) Studied elements Model 1

(d) Elevation Model 2 (e) Plan Model 2 (f) Studied elements Model 2

Fig. 1 Elevation, plan and element location for Models 1 and 2

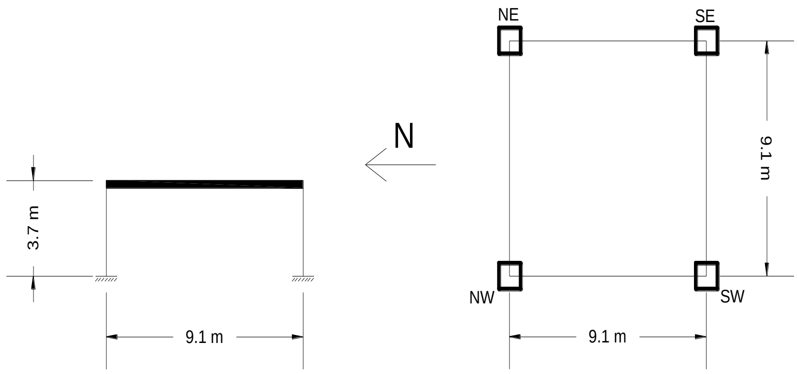

(a) Elevation (b) Plan

Fig. 2 Elevation and plan of the equivalent SDOF models (Models 1E and 2E)

rules were limited to elastic SDOF systems and that the codes do not explicitly state their applicability: it is not specified if they should be applied to simple or complex structures. In order to compare the accuracy of the rules for different structural representations, the accuracy of the rules is also studied for *equivalent* SDOF systems. One equivalent SDOF model is considered for each steel building. These systems have a SDOF in each horizontal direction. They will be denoted hereafter as Model 1E and Model 2E. The elevation and plan of these systems are shown in Fig. 2. The weight of the *equivalent* SDOF system is the same as the total weight of its corresponding MDOF system and its lateral stiffness is selected in such a way that its natural period is the same as the fundamental natural period of its corresponding MDOF system. In order to have the equivalence in both horizontal directions, square hollow structural sections were used for columns. They were HSS26×26×1/2 and HSS22×22×1/2 for the equivalent 3- and 10-level models, respectively. The damping ratio and the yielding strength are selected to be the same for the SAC and the equivalent SDOF models. The yielding strength was determined from a pushover analysis. It must be noted that in a strict sense, the simpler models are not the typical SDOF systems studied in the structural dynamics textbooks since axial forces can be developed in the columns under the action of horizontal excitations. The axial force importantly define the plastic hinge formation which, as stated earlier, have an important effect on the dissipated energy and consequently in the structural response.

3.3 Earthquake loading

Dynamic responses of a structure excited by different earthquake time histories, even when they are normalized in terms of the peak ground acceleration or in terms of any other parameter, are expected to be different, reflecting their different frequency contents. Thus, evaluating structural responses excited by an earthquake may not reflect the behavior properly. To study the responses of the models comprehensively and to make meaningful conclusions, they are excited by twenty recorded earthquake motions in time domain with different frequency contents, recorded at different locations. The horizontal components of the earthquakes are arranged in such a way that the component with largest peak in its response spectra, in terms of pseudo accelerations, are applied in the E-W direction and the other one in the N-S direction. The earthquake records are scaled in terms

Table 2 Earthquake models

No	DATE	STATION	T (seg)	EPICENTER (km)	DEPTH (km)	MAGNITUDE	PGA (cm/s²)
1	09/06/80	Cerro Prieto	0.12	20	4	6.30	308
2	02/09/07	Lake MathewsDam	0.15	13	12	4.70	507
3	02/09/05	Salton Sea WildlifeRefuge	0.19	2	9	4.84	236
4	27/08/11	Bear Valley, WebbResidence	0.21	13	7	4.62	239
5	06/04/12	Paicines, HainHomestead	0.23	3.8	5	4.00	232
6	28/09/04	Parkfield, Eades	0.24	9.8	7	6.00	384
7	16/06/05	Redlands, SevenOaksDam	0.25	10	11	5.50	290
8	30/12/09	Holtville	0.26	42	6	5.80	322
9	09/08/07	Granada Hills, PorterRanch	0.27	6	7	4.60	148
10	18/05/09	Compton, Cressey Park	0.30	9	15	4.65	207
11	12/06/05	Mountain Center, PineMeadows R.	0.31	5	14	5.20	200
12	18/02/04	Cobb	0.32	2	3	4.40	213
13	31/10/07	San Jose, PrivateResidence	0.35	10	9	5.40	199
14	02/03/07	Martinez, VA Medical Clinic	0.39	10	16	4.40	149
15	22/12/03	San Luis Obispo, Rec. Center	0.40	61	7	6.40	162
16	04/04/10	CalexicoFireStation	0.40	62	10	7.20	266
17	07/07/10	Mountain Center, PineMeadows R.	0.75	20	11	5.43	185
18	28/06/92	Morongo Valley FireStation	0.81	28	5	6.50	198
19	28/02/01	Olympia, WDOTHighway Test Lab	0.82	18	59	6.80	250
20	10/01/10	Ferndale, LostCoastRanch	0.88	36	21	6.50	352

of the spectral acceleration in the fundamental mode of vibration of the structure ($S_a(T_1)$), taking as a reference the component with the largest response spectra; the other components were scaled with the same factors. The building models behave essentially elastic under the action of any of the records, then, in order to have inelastic behavior, the earthquake records are uniformly scaled up in such a way that for the critical earthquake the models develop a collapse mechanism or a maximum interstory displacement of about 1.8% (whatever occurs first). The characteristics of the earthquakes are given in Table 2. As shown in the table, the predominant periods of the earthquakes vary from 0.12 to 0.88 sec. The predominant period for each earthquake is defined as the period where the largest peak in the pseudo-acceleration elastic response spectrum occurs. The earthquake time histories were obtained from the Data Sets of the National Strong Motion Program (NSMP) of the United States Geological Surveys (USGS). Additional information on these earthquakes can be obtained from these data base.

4. Combination rules and loading cases

4.1 Combination rules

The combination rules are formally defined in this section. For the ease of discussion, R_X will represent hereafter the maximum absolute load effect at a particular location when the structure is excited by the horizontal *X* component of a given earthquake. Similarly, R_Y and R_Z will denote the corresponding maximum absolute load effect at the same location when the structure is excited by the horizontal *Y* and the vertical component of the earthquake, respectively. The load effects produced by each component can be calculated using many simplified methods including the equivalent lateral load procedure, modal analysis, and time history analysis. Then, the combined effect can be calculated as the most unfavorable of

$$R_{C1} = R_X + \lambda R_Y + \lambda R_Z \tag{1a}$$

$$R_{C1} = \lambda R_X + R_Y + \lambda R_Z \tag{1b}$$

$$R_{C1} = \lambda R_X + \lambda R_Y + R_Z \tag{1c}$$

The above equations represent the *Percentage Rule*, if λ=0.3 is used, it represents the 30% rule for three components. According to the *SRSS* rule the combined response is given by

$$R_{C2} = \sqrt{R_X^2 + R_Y^2 + R_Z^2} \tag{2}$$

As stated earlier, in codes, the combination rules are generally stated to combine the two horizontal components. To study the combinations rules only for the two horizontal components, Eqs. (1) and (2) can be modified as

$$R_{C1} = R_X + \lambda R_Y \tag{3a}$$

$$R_{C1} = \lambda R_X + R_Y \tag{3b}$$

$$R_{C2} = \sqrt{R_X{}^2 + R_Y{}^2} \tag{4}$$

The basic assumption of the *SRSS* rule is that there is no correlation between the horizontal components and between their effects. The validity of this assumption is evaluated in light of the results of this study. These rules seem to be simple to apply. However, they need critical review with respect to the issues raised earlier. By assuming the responses to be either elastic or inelastic, the *best estimate* of the response can be obtained by simultaneously applying the three (or the two horizontal) normal or principal components, then the accuracy of the combination rules is estimated. By considering several incidence angles of the components the critical response can also be estimated.

4.2 Loading cases

To meet the objectives of the study, *the best estimate* of the responses (also called the *reference responses*) of the two models when excited by the normal or principal components of all 20 earthquakes are needed. The responses produced by a harmonic excitation of the base are also needed. For the ease of discussion, the following notations will be used in the remainder of the paper. Considering the three components of an earthquake, the *first horizontal component* will be denoted as *X*, the *second horizontal component* as *Y*, and the vertical component as *Z*. The symbols X_n, Y_n, and Z_n will indicate that the structures are excited by the normal components, and X_p, Y_p and

Z_p will indicate that the principal components are used instead. Hence, the notations (X_n, Y_n, Z_n) indicate that the structure is excited by the *first*, *second* and *third* normal components applied simultaneously to the *N-S*, *E-W* and the vertical directions of the structure, respectively. To obtain the reference responses when excited by the three normal and principal components, the following four load cases are considered:

Case 1: responses when the models are excited by (X_n, Y_n, Z_n).

Case 2: same as *Case 1*, but the horizontal components are interchanged (Y_n, X_n, Z_n).

Case 3: same as *Case 1* but the principal components are used instead (X_p, Y_p, Z_p).

Case 4: same as *Case 3* but the horizontal components are interchanged (Y_p, X_p, Z_p).

To obtain the reference responses when excited by the two horizontal normal and principal components, the following additional four load cases are considered:

Case 5: responses when the models are excited by (X_n, Y_n, *0*).

Case 6: same as *Case5* but the horizontal components are interchanged (Y_n, X_n, *0*).

Case 7: same as *Case 5*, but the models are excited by the principal components (X_p, Y_p, *0*).

Case 8: same as *Case 7* but the horizontal components are interchanged (Y_p, X_p, *0*).

As mentioned earlier, axial loads (collinear) and interstory shear (non-collinear) are considered to be the response parameters in this study. The *reference response* when excited by the three normal components, denoted hereafter as R_{n3} is considered to be the maximum response of Cases *1* and *2*, while the *reference response* for the three principal components, denoted as R_{p3}, is considered to be the maximum response of Cases *3* and *4.* Similarly, the *reference response* for the two horizontal components, denoted as R_{n2}, is considered to be the maximum response of *Cases 5* and *6* for the normal components. The corresponding reference response for the principal components, R_{p2}, is the maximum response of *Cases 7* and *8*.

To obtain the responses according to the combinations rules when excited by the three (or the two) normal or principal components, the following four load cases are considered:

Case 9: responses according to the *30%* and the *SRSS* combination rules when excited by (a) (X_n, *0, 0*), (b) (*0*, Y_n, *0*), and (c) (*0, 0*, Z_n).

Case 10: same as *Case 9*, but the horizontal components are interchanged; (a) (Y_n, *0, 0*), (b) (*0*, X_n, *0*), and (c) (*0, 0*, Z_n).

Case 11: same as *Case 9,* but the principal components are used instead; (a) (X_p, *0, 0*), (b) (0, Y_p, *0*), and (c) (*0, 0*, Z_p).

Case 12: same as *Case 11* but the horizontal components are interchanged; (a) (Y_p, *0, 0*), (b) (0, X_p, *0*), and (c) (*0, 0*, Z_p).

For harmonic excitation of the base, the applied *first* and *second horizontal components* are denoted as P_X and P_Y. This loading is completely defined in Section 8 of the paper. The required analyses are:

Case *13*, the structures are simultaneously excited by the two harmonic components; the first component is acting along the *N-S* structural direction and the second along the other horizontal structural direction (*E-W*). This case is denoted as (P_X, P_Y, *0*).

Case *14*, same as Case *13*, but the components are interchanged (P_Y, P_X, *0*).

Case *15*, the total response according to the *30%* and the *SRSS* combination rules considering the following two sub-cases: a) (P_X, *0, 0*) and b) (0, P_Y, *0*).

Case 16, the total response according to the *30%* and the *SRSS* combination rules considering the following two sub-cases: a) (P_Y, *0, 0*) and b) (0, P_X, *0*).

Thus, for two structures, twenty earthquakes, sixteen seismic loading cases, and considering elastic and inelastic analysis, a total of 1280 analyses of complex MDOF structures, with several thousands of degrees of freedom, under seismic loading are required. For the estimation of the critical incidence angle the horizontal components are rotated at each 5^o. In this case a total of 1440 analysis of complex MDOF systems are additionally required. Moreover, for harmonic loading several hundred of complex analysis of MDOF systems are required too. Thus, without considering the seismic analysis of simplified SDOF systems, more than 3000 seismic analysis of complex MDOF systems were performed.

5. Critical response

To study the critical orientation, responses are estimated for normal and principal components. The response parameters are also estimated for the normal components rotated at each 5^o, varying the rotation angle from 0^o to 90^o. Then, the *R* parameter, defined as the ratio of the response produced by the normal (or by the rotated normal components) to that of the principal components, is calculated. Thus, if a value of *R* is larger than unity for a particular case, it implies that the maximum response is produced by the normal or rotated normal components, while a value of *R* smaller than unity implies that the maximum response is produced by the principal components. The R parameter is estimated for the two models, the twenty earthquakes, local (axial load) and global (interstory shear) response parameters, and elastic and inelastic behavior. Although the study is made for two and three components the results are presented only for three components because of lack of space.

5.1 Axial load

The *R* values for the axial loads acting on some columns of the base (Figs. 1(c) and (f)) are calculated, as stated earlier, for several cases, however, the plots are presented only for a few cases. The *R* parameter corresponding to Earthquakes 3, 6, 9,12, 15 and 18 are presented in Figs. 3(a), 3(b), 3(c), 3(d), 3(e) and 3(f), respectively, for Model 1 and elastic behaviour. The plots clearly indicate that the *R* parameter significantly may vary with the particular earthquake being considered and the locations of the structural elements. The *R* values, for columns of MRF may increase or decrease with the incidence angle without showing any pattern. It is also noted that, for a given earthquake, the incidence angle corresponding to the maximum value of *R*, which defines the maximum axial load, is in general different for each column. The most important observation that can be made is that, in many cases, the maximum value of *R* is larger than unity indicating that the maximum response, in terms of axial loads, may be larger than that produced for the principal components; values of up to 1.40 are observed. For the case of columns of GF, the variation of *R* with the incidence angle is much smaller than that of columns of MRF. The reason for this is that the effect of the horizontal components on the axial load of these columns is much smaller.

The peak or maximum values of *R* for all the earthquakes and their statistics, in terms of the mean and coefficient of variation, averaged over all the earthquakes are given in Table 3. As observed earlier from the plots presented in Fig. 3, the peak values of *R* significantly vary from one earthquake to another and from one column to another. The mean and COV values of *R*, considering all models, columns and earthquakes are 1.04 and 0.21, respectively, indicating that on an average basis, the critical axial load is very close to that produced by principal components and that the uncertainty in the estimation is moderate.

In order to study the effect of inelastic behavior on the *R* parameter, the recorded motions were

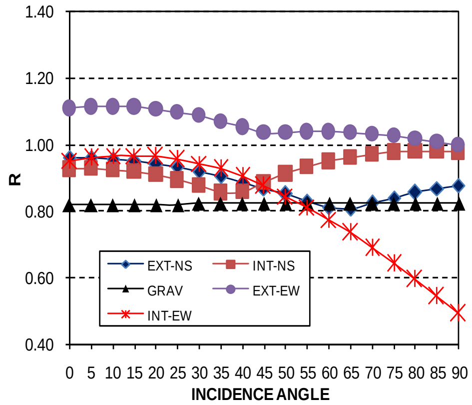

(a) Earthquake 3

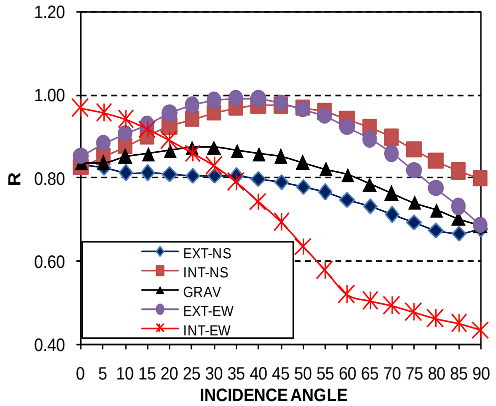

(b) Earthquake 6

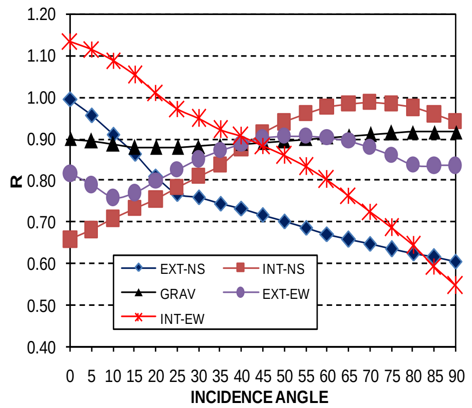

(c) Earthquake 9

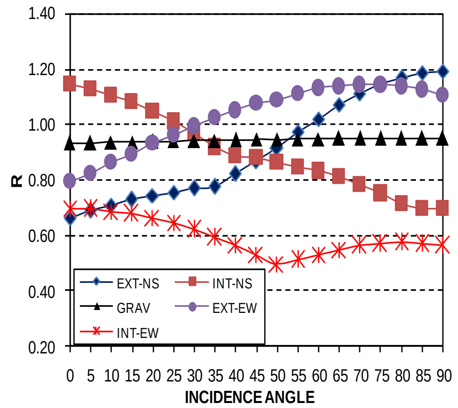

(d) Earthquake 12

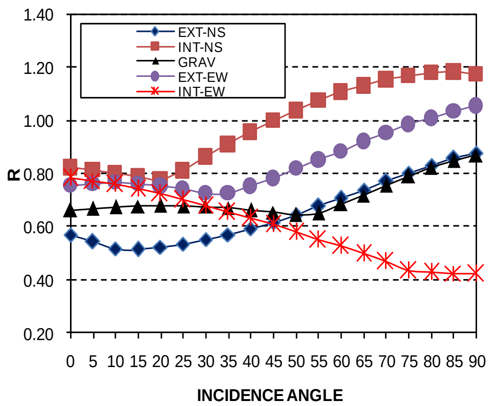

(e) Earthquake 15

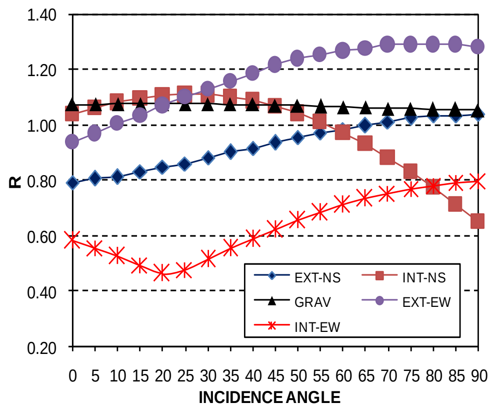

(f) Earthquake 18

Fig. 3 Ratio (R) of axial load of rotated components to that of principal components, Model 1 and elastic behavior

scaled in terms of $S_a(T_1)$ in such a way that significant yielding occurred under the critical earthquake, as commented before. It was observed that about nine to nineteen plastic hinges were formed in the models. Plots for *R* similar to those previously discussed for elastic behaviour are developed. The results for Model 1 are given in Figs. 4(a), 4(b), 4(c), 4(d), 4(e) and 4(f), for Earthquakes 3, 6, 9, 12, 15 and 18, respectively. As for the elastic case, the *R* values for columns of MRF, in general, significantly vary from one column to another, from one earthquake to another and from one incidence angle to another without showing any trend. For columns of GF the *R* parameter is essentially constant for all incidence angles. The most important observation that can be made is that the peak values of *R* are, in general, much larger for inelastic behaviour, values close to 3 are observed in some cases. The peak values and statistics of *R* for inelastic behaviour are shown in Table 4. The mean values are significantly larger for the inelastic case, values larger than 2 are observed in some cases. The uncertainty in the estimation significantly increases while changing from elastic to inelastic behaviour, particularly for Model 1.

The R values and the uncertainty in their prediction for two (horizontal) are essentially the same than those of three components, for elastic behaviour. For inelastic behaviour, however, the mean values and the COV increase by about 15% and 30% when only the two horizontal components are considered.

Table 3 Statistics for the *R* parameter, axial load, elastic behavior

No	MODEL 1					MODEL 2				
	EXT-NS	INT-NS	GRAV	EXT-EW	INT-EW	EXT-NS	INT-NS	GRAV	EXT-EW	INT-EW
1	0.99	1.06	1.02	1.01	1.28	1.02	1.03	1.08	0.67	1.00
2	0.97	1.01	0.96	1.12	0.63	1.11	0.96	0.80	1.83	0.97
3	0.96	0.98	0.82	1.11	0.97	0.78	0.80	0.58	1.34	0.81
4	1.07	0.94	1.35	0.89	0.93	0.69	0.87	0.99	0.83	0.87
5	1.03	1.04	1.03	1.15	1.03	0.94	1.00	0.90	1.63	1.00
6	0.83	0.97	0.87	0.99	0.97	1.13	1.01	1.00	1.76	1.02
7	0.80	0.97	0.93	0.97	0.95	1.05	1.02	1.02	1.43	1.01
8	0.92	1.00	0.96	1.05	0.61	1.01	0.99	0.99	2.03	1.01
9	1.00	0.99	0.92	0.91	1.14	0.64	1.06	1.25	1.04	1.07
10	1.05	1.04	1.02	1.04	1.04	1.09	1.00	0.99	1.26	1.00
11	1.24	1.03	1.08	1.06	1.20	0.65	1.17	1.14	0.68	1.21
12	1.19	1.15	0.95	1.14	0.70	0.80	1.09	0.97	1.35	1.13
13	1.01	1.00	0.99	1.01	0.76	1.01	0.98	1.06	1.89	0.98
14	1.13	1.09	1.13	1.05	1.28	0.65	0.98	0.98	1.19	1.00
15	0.88	1.18	0.87	1.06	0.79	0.85	1.03	0.93	1.45	1.06
16	0.97	1.05	1.08	1.07	0.84	1.05	1.04	0.96	1.82	1.06
17	0.93	1.04	0.95	1.13	0.61	1.07	0.99	0.88	1.68	1.00
18	1.04	1.11	1.08	1.29	0.80	1.08	0.93	1.75	1.14	0.97
19	1.01	0.99	1.00	1.16	0.92	1.10	1.01	0.83	1.64	1.03
20	1.08	1.20	1.03	1.27	1.17	1.22	1.02	1.01	1.49	1.07
$\boldsymbol{\mu}$	1.01	1.04	1.00	1.07	0.93	0.95	1.00	1.01	1.41	1.01
COV	0.11	0.07	0.11	0.10	0.23	0.19	0.08	0.22	0.28	0.08
$\boldsymbol{\mu}$(ALL)=1.04 **COV**(ALL)=0.21										

Table 4 Statistics for the *R* parameter, axial load, inelastic behavior

No	MODEL 1					MODEL 2				
	EXT-NS	INT-NS	GRAV	EXT-EW	INT-EW	EXT-NS	INT-NS	GRAV	EXT-EW	INT-EW
1	1.63	1.09	1.05	1.30	1.01	1.17	1.05	1.42	1.10	1.01
2	1.08	0.89	1.29	1.16	1.06	1.02	1.29	1.15	0.93	1.02
3	2.12	1.50	0.93	1.26	1.21	1.25	0.74	0.87	0.94	0.74
4	1.35	1.03	1.39	1.52	1.12	1.03	1.52	1.44	0.88	1.50
5	1.35	1.49	1.03	1.59	2.42	1.13	1.03	1.04	1.03	1.03
6	1.09	0.97	1.09	1.33	1.04	1.18	1.48	0.79	1.22	0.42
7	2.23	1.57	1.54	1.22	1.37	1.08	2.26	1.14	0.94	1.31
8	1.55	0.98	1.01	2.94	1.58	1.03	1.04	1.00	2.45	1.86
9	1.92	1.04	1.30	1.26	1.30	0.94	1.58	1.52	1.21	2.33
10	1.00	1.42	1.19	1.67	0.95	1.34	2.90	1.39	2.01	2.70
11	2.31	1.27	1.67	2.75	1.31	1.30	1.61	0.80	1.24	1.53
12	1.16	1.11	1.01	1.53	1.33	1.37	1.20	0.96	1.25	0.96
13	1.24	1.04	1.05	1.17	1.04	1.04	1.03	1.31	1.00	1.01
14	1.58	1.06	1.27	1.01	1.74	1.36	1.82	1.18	1.89	2.02
15	1.41	1.21	0.97	1.68	1.18	1.08	1.68	1.06	1.18	1.38
16	1.52	1.10	1.34	1.90	1.12	1.16	1.34	1.23	0.93	1.07
17	1.08	1.38	1.15	0.71	1.30	1.26	1.42	1.21	1.01	1.59
18	1.81	1.15	1.49	2.05	1.27	1.18	1.31	2.18	1.16	1.34
19	1.52	0.97	0.94	0.77	1.11	1.15	1.34	0.83	1.11	1.20
20	0.99	1.23	1.04	1.22	0.99	1.12	1.42	1.44	1.03	1.49
μ	1.50	1.18	1.19	1.50	1.27	1.16	1.45	1.20	1.23	1.38
COV	0.27	0.17	0.18	0.38	0.26	0.11	0.33	0.27	0.34	0.39
μ(ALL)=1.30 **COV**(ALL)=0.31										

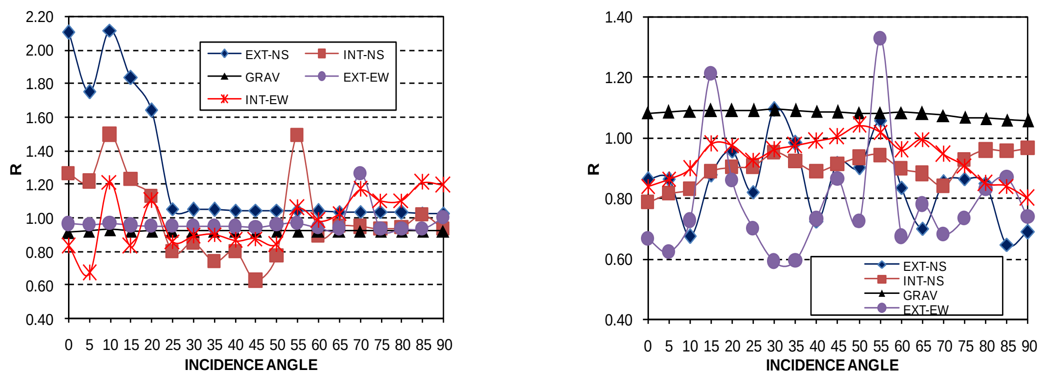

(a) Earthquake 3 (b) Earthquake 6

Fig. 4 Ratio (R) of axial load of rotated components to that of principal components, Model 1 and inelastic behavior

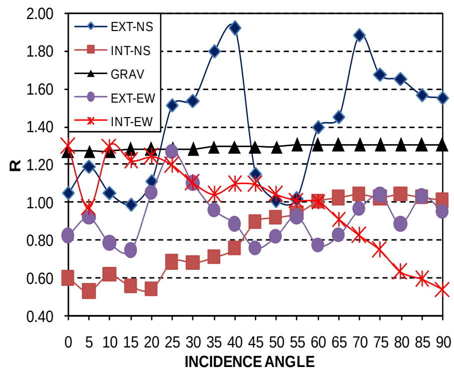

(c) Earthquake 9

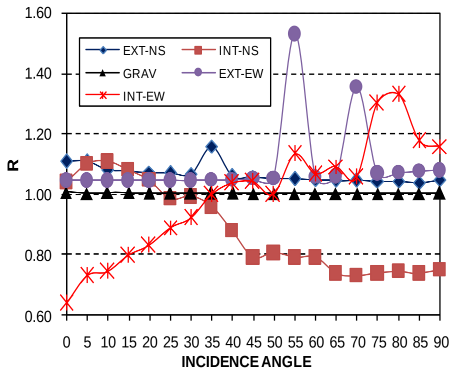

(d) Earthquake 12

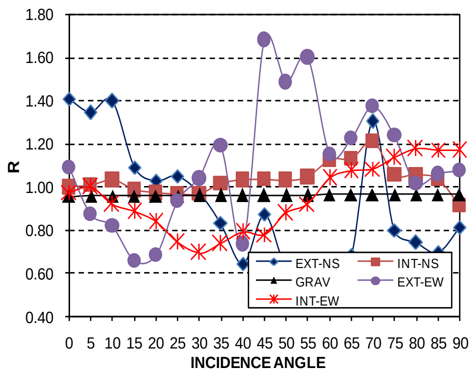

(e) Earthquake 15

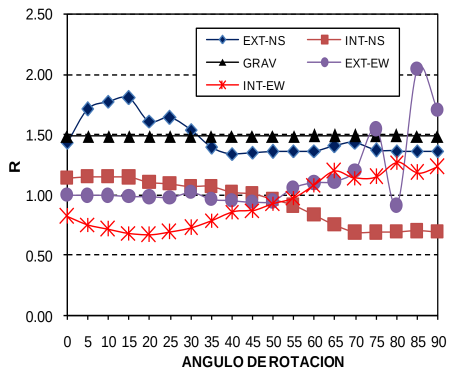

(f) Earthquake 18

Fig. 4 Continued

5.2 Interstory shear

The R parameter for interstory shears is now discussed. The shear for a given interstory in the X direction produced by the simultaneous application of the three components is denoted as V_x. Similarly, the interstory shear in Y direction produced by the simultaneous application of the three components is denoted as V_y. Then, the *total interstory shear* V_R, is calculated as $V_R = \sqrt{Vx^2 + Vy^2}$. As for the case of axial load, a value of V_R is calculated for normal components, for rotated normal components at several incidence angles, and for principal components. The ratio of V_R for normal (or rotated normal components) to that of principal components will give the R ratio for interstory shear. Similar plots to those of Figs. 3 and 4, developed for axial loads, were also developed for interstory shears for both models and type of behaviors, but are not shown, only the statistics are reported. The results are presented in Tables 5 and 6 for elastic and inelastic behaviors. Results indicate that, unlike the case of axial loads, the variation of V_R from one earthquake to another and from one story to another is small. For elastic behavior the mean value is 1.02 for Model 1 and 1.01 for Model 2. The COV is 0.03 for both models. For inelastic behavior, the V_R mean values are 1.06 and 1.09 for Models 1 and 2, respectively, while the corresponding values for COV are 0.08 and 0.12, indicating a small dispersion. There are no significant differences between the statistics of R for two and three components, for both elastic and inelastic behavior.

Table 5 Statistics for the *R* parameter, interstory shear, elastic behavior

No	MODEL 1			MODEL 2								
	ST 3	ST 2	BASE	ST 9	ST 8	ST 7	ST 6	ST 5	ST 4	ST 3	ST 2	BASE
1	1.02	0.99	1.00	0.99	0.99	0.99	0.98	1.01	1.00	1.00	0.99	1.01
2	0.97	1.02	1.02	0.99	0.99	0.99	0.99	0.99	0.99	0.99	0.99	0.99
3	1.02	1.01	1.01	0.99	0.99	0.99	0.99	1.00	1.00	1.00	0.98	0.95
4	1.02	0.92	1.06	0.90	0.87	0.90	0.90	0.91	0.92	0.92	0.93	0.93
5	0.97	1.06	1.02	1.00	1.03	1.02	1.01	0.99	1.00	1.00	1.00	1.00
6	1.01	0.98	0.99	1.05	1.06	1.05	1.03	1.03	1.03	1.02	1.02	1.02
7	1.03	1.06	0.99	1.06	1.06	1.07	1.05	1.05	1.04	1.03	1.04	1.02
8	1.01	1.00	0.99	1.00	1.00	1.00	1.00	1.00	1.01	1.00	1.01	1.00
9	0.98	1.00	0.99	1.00	1.00	1.01	1.02	1.00	1.01	1.00	1.00	1.00
10	1.02	1.00	1.01	1.01	1.00	1.00	1.00	1.00	1.00	1.00	1.00	1.00
11	1.06	1.04	1.06	1.08	1.00	1.03	1.03	1.00	0.97	0.98	0.98	0.99
12	1.10	1.02	1.11	1.01	1.00	1.00	0.99	0.99	0.99	1.00	1.01	1.01
13	1.03	1.00	1.03	1.01	1.01	1.01	1.01	1.01	1.01	1.01	1.01	1.01
14	1.01	1.01	1.03	1.00	1.00	1.01	1.01	1.00	1.00	1.00	1.00	0.99
15	1.03	1.01	0.98	1.01	1.00	1.00	1.01	1.00	1.01	1.01	1.02	1.01
16	0.98	0.99	1.05	1.06	1.08	1.05	0.98	1.01	1.04	1.06	1.06	1.07
17	1.02	1.02	1.01	1.01	1.01	1.01	1.02	1.02	1.01	1.01	1.00	1.00
18	1.00	1.04	1.06	1.03	1.02	1.02	1.03	1.00	1.00	1.00	1.08	1.07
19	1.02	1.03	1.04	1.03	1.03	1.03	1.03	1.03	1.03	1.02	1.02	1.02
20	1.02	1.03	1.07	1.02	1.03	1.02	1.01	1.01	1.01	1.01	1.01	1.01
$\boldsymbol{\mu}$	1.02	1.01	1.03	1.01	1.01	1.01	1.00	1.00	1.00	1.00	1.01	1.01
COV	0.03	0.03	0.03	0.04	0.04	0.03	0.03	0.03	0.03	0.03	0.03	0.03
$\boldsymbol{\mu}$(ALL)=1.01 **COV**(ALL)=0.03												

Table 6 Statistics for the *R* parameter, interstory shear, inelastic behavior

No	MODEL 1			MODEL 2								
	ST 3	ST 2	BASE	ST 9	ST 8	ST 7	ST 6	ST 5	ST 4	ST 3	ST 2	BASE
1	1.03	1.00	1.04	0.98	0.97	0.98	0.98	1.05	0.98	1.01	0.99	1.04
2	1.03	0.97	0.95	1.25	1.22	1.17	1.14	1.11	1.08	1.08	1.13	1.08
3	1.15	1.18	1.19	1.03	1.04	1.05	1.02	1.05	1.05	1.09	1.10	1.07
4	1.08	0.98	1.01	0.93	0.86	0.93	0.92	0.89	0.98	0.98	1.07	0.98
5	1.24	1.45	1.25	1.05	1.20	1.14	1.08	1.09	1.14	1.10	1.13	1.05
6	1.04	1.04	1.02	1.19	1.18	1.19	1.14	1.08	1.09	1.10	1.11	1.14
7	1.04	1.09	1.06	1.04	1.02	1.05	1.05	1.07	1.06	1.00	1.09	1.07
8	1.03	1.01	1.01	1.11	1.15	1.20	1.16	1.11	1.10	1.08	1.13	1.10
9	1.11	1.11	1.18	0.96	0.97	1.00	1.03	0.99	1.01	1.03	0.97	0.96
10	1.02	1.03	1.08	1.52	1.39	1.61	1.43	1.45	1.53	1.79	1.34	1.66
11	0.99	1.15	1.08	1.09	1.03	1.05	0.93	0.88	0.98	1.02	1.04	0.91

Table 6 Continued

No	MODEL 1			MODEL 2								
	ST 3	ST 2	BASE	ST 9	ST 8	ST 7	ST 6	ST 5	ST 4	ST 3	ST 2	BASE
12	1.06	1.06	1.17	0.98	0.99	1.08	1.09	1.08	1.07	1.09	1.13	1.06
13	1.03	1.00	1.04	1.08	1.10	1.13	1.09	1.05	1.06	1.01	1.03	1.05
14	1.16	1.09	1.11	1.33	1.27	1.18	1.20	1.33	1.10	1.11	1.11	1.10
15	1.05	0.98	0.93	1.09	1.08	1.06	1.03	1.04	1.02	1.01	1.02	1.02
16	1.01	1.03	1.05	1.09	1.09	1.09	1.09	1.03	1.08	1.03	1.10	1.10
17	0.97	1.06	1.03	1.17	1.19	1.15	1.15	1.11	1.08	1.07	1.10	1.10
18	1.05	1.05	1.03	1.07	1.03	1.05	1.04	1.07	1.03	1.06	1.11	1.09
19	1.07	1.05	1.06	1.06	1.05	1.14	1.17	1.11	1.09	1.08	1.11	1.09
20	1.02	1.03	1.02	1.03	1.05	1.02	1.05	1.01	1.01	0.99	0.98	1.02
$\boldsymbol{\mu}$	1.06	1.07	1.07	1.10	1.09	1.11	1.09	1.08	1.08	1.09	1.09	1.08
COV	0.06	0.10	0.08	0.13	0.11	0.12	0.10	0.12	0.11	0.16	0.07	0.13
$\boldsymbol{\mu}$(ALL)=1.08 **COV**(ALL)=0.12												

In summary, the mean value of the R parameter and the uncertainty in its estimation are larger for axial loads than for interstory shears, and larger for inelastic that for inelastic behavior. The critical axial load or interstory shear occurs for an incidence angle different than that of normal or principal components. It is proposed that the critical response be obtained as 1.40 and 1.10 times that of principal components, for axial load and interstory shears, respectively, for the structural system under consideration.

6. Accuracy of the combination rules for complex MDOF systems

The accuracy of the rules in the estimation of the combined response is now discussed. Both, global and local response parameters are considered. Only the results for the three components are presented because of lack of space, even though the results for the two horizontal components are also calculated and briefly discussed.

6.1 30% rule, elastic behavior

The results for axial loads are first presented. Considering the excitations given by *Case 9* of loading, three possible combined responses can be calculated for axial load and normal components as: ${}^9X_n$+0.3${}^9Y_n$+0.3${}^9Z_n$, 0.3${}^9X_n$+${}^9Y_n$+0.3${}^9Z_n$ and 0.3${}^9X_n$+0.3${}^9Y_n$+${}^9Z_n$, where ${}^9X_n$, ${}^9Y_n$ and ${}^9Z_n$ are defined as the responses produced for Cases *3a*, *3b* and *3c*, respectively. The larger of the three combined responses when normalized with respect to the *reference response* (R_{n3}) defined earlier will give a random variable defined as ${}^9R_{n3,30}$. By using the same procedure for Load Case *10*, the ${}^{10}R_{n3,30}$ parameter can be calculated. The combination of both cases (${}^9R_{n3,30}$ and ${}^{10}R_{n3,30}$) and 20 earthquakes give a total of 40 sample points. It will be denoted as the random variable $R_{n3,30}$. Following exactly the same procedure for principal components (excitations given by load Cases 11 and 12), 40 sample points are similarly generated, which will be denoted by the random variable $R_{p3,30}$. Typical results for the $R_{n3,30}$ parameter are given in Figs. 5(a) and 5(b) for Model 1. The results indicate that $R_{n3,30}$ significantly varies with the particular earthquake being considered and the locations of the elements without showing any trend. For most of the cases the combined response is underestimated. The results for $R_{p3,30}$ follow a similar trend.

The accuracy of the 30% combination rule in the estimation of interstory shear is discussed next. The parameters ${}^{9}X_n$, ${}^{9}Y_n$, ${}^{9}Z_p$, and so on, as well as $R_{n3,30}$ and $R_{p3,30}$, have a similar meaning

Table 7 Statistics for $R_{n3,30}$, $R_{p3,30}$, $R_{n3,SRSS}$ and $R_{p3,SRSS}$ for MDOF systems and earthquake loading, axial load and interstory shear, elastic behavior

MODEL (1)	LOCATION (2)		30% RULE				SRSS RULE				Sample Size (11)
			Normal $R_{n3,30}$		Principal $R_{p3,30}$		Normal $R_{n3,SRSS}$		Principal $R_{p3,SRSS}$		
			Mean (3)	COV (4)	Mean (5)	COV (6)	Mean (7)	COV (8)	Mean (9)	COV (10)	
1	AXIAL LOAD	INT-NS	0.89	0.21	0.93	0.23	0.89	0.24	0.92	0.22	40
		EXT-NS	0.87	0.23	0.89	0.19	0.83	0.23	0.86	0.19	40
		GRAV	1.01	0.04	1.03	0.03	1.00	0.03	1.00	0.02	40
		INT-EW	0.91	0.30	0.80	0.38	0.88	0.31	0.78	0.38	40
		EXT-EW	0.88	0.28	0.93	0.23	0.84	0.28	0.90	0.24	40
		ALL	**0.91**	**0.23**	**0.92**	**0.24**	**0.89**	**0.24**	**0.89**	**0.24**	200
	SHEAR	ST3	1.07	0.17	1.06	0.09	1.08	0.17	1.08	0.09	40
		ST2	1.06	0.13	1.08	0.09	1.08	0.14	1.10	0.09	40
		BASE	1.04	0.14	1.08	0.08	1.05	0.14	1.09	0.08	40
		ALL	**1.06**	**0.14**	**1.07**	**0.08**	**1.07**	**0.15**	**1.09**	**0.09**	**120**
2	AXIAL LOAD	INT-NS	0.91	0.15	0.84	0.24	0.88	0.17	0.79	0.26	40
		EXT-NS	0.95	0.14	0.95	0.16	0.94	0.15	0.91	0.16	40
		GRAV	1.01	0.03	1.01	0.01	1.00	0.02	1.00	0.01	40
		INT-EW	0.93	0.16	0.84	0.24	0.90	0.17	0.81	0.24	40
		EXT-EW	0.86	0.19	0.94	0.18	0.84	0.18	0.91	0.18	40
		ALL	**0.93**	**0.15**	**0.92**	**0.19**	**0.91**	**0.16**	**0.88**	**0.20**	200
	SHEAR	ST10	1.10	0.12	1.03	0.17	1.13	0.13	1.05	0.16	40
		ST9	1.12	0.12	1.00	0.13	1.14	0.12	1.02	0.13	40
		ST8	1.12	0.08	1.03	0.12	1.14	0.09	1.04	0.12	40
		ST7	1.09	0.09	1.01	0.18	1.12	0.09	1.02	0.17	40
		ST6	1.09	0.09	1.04	0.13	1.12	0.09	1.04	0.13	40
		ST5	1.09	0.09	1.02	0.15	1.12	0.10	1.03	0.15	40
		ST4	1.11	0.09	1.03	0.18	1.14	0.09	1.03	0.18	40
		ST3	1.12	0.10	1.01	0.18	1.15	0.10	1.02	0.18	40
		BASE	1.12	0.09	1.03	0.17	1.15	0.09	1.04	0.17	40
		ALL	**1.11**	**0.10**	**1.02**	**0.16**	**1.14**	**0.11**	**1.03**	**0.16**	**360**

than that of axial load; the only difference is that now they represent interstory shear. Plots for $R_{n3,30}$ and $R_{p3,30}$ for the case of shear were also developed but are not presented; only their statistics are discussed. The statistics of $R_{n3,30}$ and $R_{p3,30}$, for both axial load and interstory shear, are summarized in Table 7. The results clearly indicate that, on an average basis, the 30% combination rule underestimates the combined axial load by about 10% and that the uncertainty associated with the estimation range between 15 and 24%, even though, as stated in Section 3.3, the earthquakes were scaled in terms of $S_a(T_1)$). One of the reasons for this uncertainty is the inherent stochastic nature of earthquake load. Another factor is related to the effects of the frequency contents of the earthquakes and the contribution of higher modes on the structural responses. In addition, collinear local response parameters like axial load on columns are affected by the action of the three components. The contribution of each component to the axial load on an specific column during some periods of time may be in phase each other but for some others may be out of phase. Due to the inherent stochastic nature of earthquake, this effect may be significantly different from one earthquake record to another. For shear, unlike the case of axial load, both rules reasonably overestimate the combined interstory shear. The overestimation is about 10% and it is observed to be essentially the same for normal and principal components.

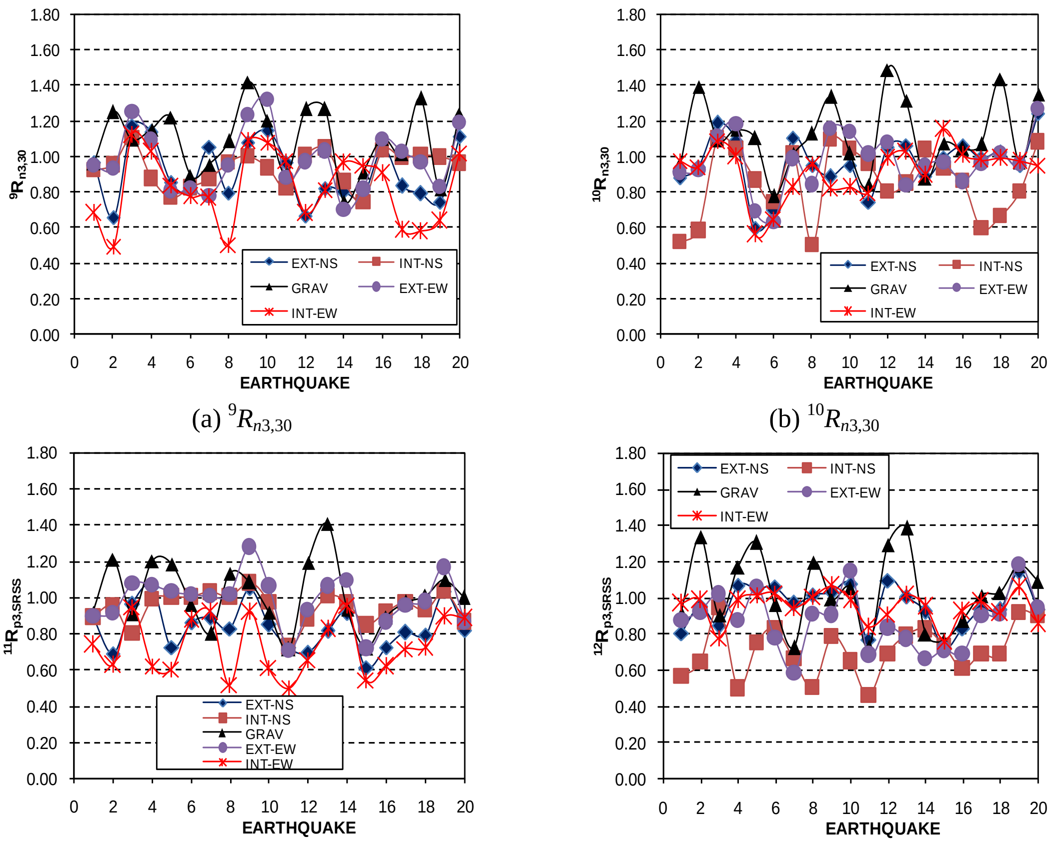

(a) $^{9}R_{n3,30}$ (b) $^{10}R_{n3,30}$

(c) $^{11}R_{p3,SRSS}$ (d) $^{12}R_{p3,SRSS}$

Fig. 5 Accuracy of the 30% and SRSS rules for MDOF systems and earthquake loading, Model 1, axial load, elastic behavior

6.2 SRSS rule, elastic behavior

The accuracy of the combined responses according to the SRSS rule is also estimated. Normalized response parameters, as those of the 30% rule, are defined for this purpose. In this case the corresponding random variables are denoted as $R_{n3,SRSS}$ and $R_{p3,SRSS}$ for normal and principal components, respectively. Typical results for $R_{p3,SRSS}$ are presented in Figs. 5(c) and 5(d). Values close to 0.4 are observed in many cases even though the components are uncorrelated. The observations made before for the 30% rule apply to this case. The fundamental statistics are presented in Table 7. The results indicate that, as for the 30% rule, on an average basis, the SRSS rule underestimate the combined axial load. The level of underestimation and the associated uncertainty are quite similar for both rules and for normal and principal components. For the case of shear, as for the 30% rule, the SRSS rule reasonable overestimates the combined response.

6.3 30% and SRSS rules, inelastic behavior

Similar plots and tables to those of elastic behavior are also developed for the 30% and SRSS rules but are not shown. Most of the conclusions made for elastic behavior essentially remain the same for inelastic behavior. The main differences are that, for the case of axial load, the values of $R_{n3,30}$, $R_{p3,30}$, $R_{n3,SRSS}$ and $R_{p3,SRSS}$ are smaller (by about 0.85) for this case indicating a larger level of underestimation of the combined response and that the uncertainty in the prediction significantly increases (about 0.30).

As stated earlier, the accuracy of the rules for the two components is also studied but the results are not presented. It can be commented, however, that the results are quite similar for two and three components. The only additional observation that can be made is that the accuracy of the rules is slightly better for three than for two components. This is particularly valid for the case of axial load. As stated in Section 6 of the paper, the accuracy of the combination rules are calculated as the ratio of the response estimated according to the rules and the reference response. It was observed from the results that, in general, these two quantities increase, in a similar proportion when the vertical component is considered, implying a larger ratio and thus a better accuracy of the rules.

From the above results it can be concluded, in general, that both the 30% and the SRSS combination rules underestimate the axial load by about 15% for normal and principal components and that the uncertainty (COV) in the underestimation can be up to 30%. These results indicate that for complex MDOF systems, there is a certain degree of correlation between the effects of individual components of earthquakes, even for the case of uncorrelated (principal) components.

6.4 Correlation between the individual effects of the horizontal components

It is implicitly assumed in the combination rules that there is no correlation between the horizontal accelerograms and between their corresponding effects. The validity of this assumption is addressed in this section of the paper; the degree of correlation between the individual effects of the horizontal components and the effect of this correlation on the accuracy of the rules are studied. The correlation is estimated for both structural models, for normal and principal components, for elastic and inelastic behavior and for collinear (axial load) and non-collinear (base shear) response parameters. Only results for axial loads on some columns of the base of Model 1 and elastic behavior are presented, however. The results for inelastic behavior of Model 1, and those corresponding to Model 2, present a similar trend.

The coefficients of correlation between the normal horizontal accelerograms (ρ_{NO}) are given in Column 2 of Table 8. Results indicate that normal components may be highly correlated. The corresponding coefficients for the principal accelerograms are obviously zero. The correlation coefficients (ρ) of the individual effects are given in Columns (3) through (12). The correlation values significantly vary from one earthquake to another and from one structural element to another. Most of the values can be considered negligible (smaller than 0.25). For many cases, however, the correlation is significant. Values of ρ larger than 0.7 are observed in some cases, even for principal components.

From the figures developed to study the accuracy of the rules and the results of Table 8, it is observed that the rules are not always inaccurate in the estimation of the combined response for correlated components. For example, from Fig. 5(a), it is observed that the 30% rule reasonably estimates the combined axial load for INT-NS, EXT-EW and GRAV Columns for Earthquake 8, even though the correlation coefficient (ρ_{NO}) of its horizontal components is 0.45. On the other hand, totally uncorrelated components are not always related to an accurate estimation of the combined response (see INT-EW Column in Fig. 5(c)). It is also observed that, for normal and

Table 8 Correlation coefficients (**ρ**) of the effect of individual components, MDOF systems and earthquake loading, axial load, elastic behavior, Model 1

No	ρ_{NO}	NORMAL COMPONENTS					PRINCIPAL COMPONENTS				
		EXT-NS	INT-NS	GRAV	EXT-EW	INT-EW	EXT-NS	INT-NS	GRAV	EXT-EW	INT-EW
(1)	(2)	(3)	(4)	(5)	(6)	(7)	(8)	(9)	(10)	(11)	(12)
1	-0.06	0.54	0.41	0.60	0.64	-0.02	0.62	0.38	0.69	0.74	-0.05
2	0.34	0.72	0.49	0.71	0.73	0.66	0.24	0.09	0.21	0.36	-0.34
3	0.07	-0.15	-0.12	-0.14	-0.14	-0.13	-0.03	0.17	0.02	0.06	-0.22
4	0.08	-0.08	-0.09	-0.07	-0.04	-0.09	0.04	0.14	0.05	0.01	0.14
5	0.35	0.47	0.38	0.48	0.49	0.42	0.20	0.26	0.23	0.18	0.18
6	0.41	0.56	0.28	0.53	0.55	0.28	-0.02	0.07	0.00	0.00	0.01
7	0.47	0.38	0.42	0.39	0.36	0.31	0.18	0.22	0.20	0.22	-0.08
8	0.45	0.36	0.22	0.34	0.31	0.25	0.18	0.15	0.17	0.27	-0.20
9	0.35	0.08	0.18	0.10	0.10	-0.04	0.12	0.23	0.16	0.15	0.22
10	0.23	-0.04	-0.02	-0.04	-0.04	-0.05	0.16	0.25	0.19	0.15	0.24
11	0.25	-0.01	-0.12	-0.03	-0.02	-0.05	0.75	0.58	0.75	0.74	-0.05
12	0.34	0.01	0.01	0.01	0.02	-0.08	0.51	0.66	0.53	0.49	-0.23
13	0.02	-0.11	-0.07	-0.09	-0.06	-0.12	-0.05	-0.01	-0.05	0.03	-0.24
14	0.25	0.22	-0.01	0.21	0.22	0.18	0.50	0.32	0.43	0.34	0.33
15	0.29	0.03	0.12	0.06	0.08	0.03	0.24	0.22	0.25	0.24	0.06
16	0.09	-0.11	0.00	-0.09	-0.10	-0.01	0.39	0.16	0.36	0.47	-0.30
17	0.19	0.28	0.05	0.25	0.21	0.33	0.13	0.07	0.13	0.26	-0.29
18	0.15	0.13	0.20	0.17	0.13	0.16	0.42	0.12	0.36	0.26	0.42
19	0.22	0.34	0.28	0.36	0.37	0.22	0.11	0.11	0.12	0.14	-0.06
20	0.04	-0.13	0.01	-0.11	-0.11	-0.06	0.45	0.34	0.50	0.55	0.00

principal components, the rules are not always inaccurate in the estimation of the combined response for large values of correlation coefficients of the individual effects, and that small values of such coefficients are not always related to an accurate estimation of combined response. The implication of this is that there are other factors that should be considered while estimating the accuracy of the combination rules.

7. Accuracy of the combination rules for equivalent SDOF systems

As for MDOF systems, the $R_{p3,30}$, $R_{p3,SRSS}$, $R_{n3,30}$ and $R_{n3,SRSS}$ parameters will represent the accuracy of the rules in the case of equivalent SDOF systems. Plots for the 30% and SRSS rules are developed for axial load and base shear, for Model 1E and 2E, for elastic and inelastic behavior, and for two and three components, but are not presented. Only the statistics for the case of three components and inelastic behavior (Table 9) are presented. The results indicate that, unlike the case of MDOF systems, both of the rules seem on an average basis to accurately estimate the combined axial load. As for the case of MDOF systems, both rules reasonably overestimate the combined base shear, the only additional observation that can be made is that the level of overestimation is slightly larger for SDOF systems. No significant differences are observed between elastic and inelastic behavior, between the 30% and the SRSS rule, or between normal and principal components.

The correlation coefficients (ρ) for axial load, only for the *NW* and *SW* columns of both the models and elastic and inelastic behavior are given in Table 10. It can be observed that, as for the case of MDOF systems, the ρ values are significant in many of the cases, even for principal components. From the results of this table and the plots (which are not presented) of $R_{p3,30}$, $R_{p3,SRSS}$,

Table 9 Statistics for $R_{n3,30}$, $R_{p3,30}$, $R_{n3,SRSS}$ and $R_{p3,SRSS}$ for SDOF systems

MODEL (1)	COLUMN LOCATION (2)		30% RULE NORMAL $R_{n3,30}$ Mean (3)	30% RULE NORMAL $R_{n3,30}$ COV (4)	30% RULE PRINCIPAL $R_{p3,30}$ Mean (5)	30% RULE PRINCIPAL $R_{p3,30}$ COV (6)	*SRSS* RULE NORMAL $R_{n3,30}$ Mean (7)	*SRSS* RULE NORMAL $R_{n3,30}$ COV (8)	*SRSS* RULE PRINCIPAL $R_{P3,30}$ Mean (9)	*SRSS* RULE PRINCIPAL $R_{P3,30}$ COV (10)	SAMPLE SIZE (11)
1E	AXIAL LOAD	NW	1.07	0.15	1.16	0.21	1.04	0.17	1.13	0.20	40
		NS	1.16	0.17	1.05	0.19	1.13	0.17	1.03	0.18	40
		NE	1.18	0.20	1.05	0.19	1.14	0.19	1.03	0.18	40
		SE	1.19	0.23	1.15	0.26	1.16	0.25	1.13	0.26	40
		ALL COLUMNS	**1.15**	**0.19**	**1.10**	**0.22**	**1.12**	**0.20**	**1.08**	**0.21**	160
	SHEAR		**1.14**	**0.08**	**1.12**	**0.07**	**1.15**	**0.09**	**1.13**	**0.08**	40
2E	AXIAL LOAD	NW	1.03	0.16	1.12	0.18	1.00	0.16	1.07	0.18	40
		NS	1.21	0.24	1.01	0.18	1.19	0.25	1.05	0.18	40
		NE	1.22	0.24	1.01	0.18	1.19	0.25	1.06	0.18	40
		SE	1.27	0.22	1.19	0.20	1.25	0.23	1.15	0.20	40
		ALL COLUMNS	**1.18**	**0.23**	**1.08**	**0.20**	**1.16**	**0.24**	**1.08**	**0.20**	160
	SHEAR		**1.11**	**0.08**	**1.11**	**0.06**	**1.13**	**0.09**	**1.11**	**0.07**	40

Table 10 Correlation coefficients (**ρ**) of the effects of individual components, SDOF systems and earthquake loading, axial load, Model 1

No	ρ_{NO}	NORMAL COMPONENTS				PRINCIPAL COMPONENTS			
		ELASTIC		INELASTIC		ELASTIC		INELASTIC	
		NW	SW	NW	SW	NW	SW	NW	SW
(1)	(2)	(3)	(4)	(5)	(6)	(7)	(8)	(9)	(10)
1	-0.06	0.40	0.18	0.52	0.52	0.40	0.18	0.69	0.69
2	0.34	0.37	0.43	0.36	0.41	0.37	0.43	0.55	0.56
3	0.07	0.10	0.03	0.07	0.07	0.10	0.03	0.03	0.05
4	0.08	0.02	0.00	0.10	0.10	0.02	0.00	0.12	0.09
5	0.35	0.14	0.25	0.36	0.41	0.14	0.25	0.11	0.11
6	0.41	0.24	0.54	0.18	0.17	0.24	0.54	0.15	0.15
7	0.47	0.12	0.39	0.43	0.44	0.12	0.39	0.08	0.09
8	0.45	0.09	0.11	0.10	0.10	0.09	0.11	0.30	0.29
9	0.35	0.23	0.21	0.14	0.14	0.23	0.21	0.31	0.26
10	0.23	0.13	0.06	0.17	0.15	0.13	0.06	0.18	0.18
11	0.25	0.08	0.01	0.38	0.37	0.08	0.01	0.44	0.45
12	0.34	0.34	0.04	0.12	0.12	0.34	0.04	0.20	0.18
13	0.02	0.23	0.36	0.34	0.35	0.23	0.36	0.52	0.52
14	0.25	0.08	0.15	0.33	0.29	0.08	0.15	0.37	0.28
15	0.29	0.04	0.08	0.01	0.01	0.04	0.08	0.08	0.08
16	0.09	0.20	0.23	0.34	0.33	0.20	0.23	0.51	0.52
17	0.19	0.05	0.33	0.16	0.17	0.05	0.33	0.30	0.29
18	0.15	0.18	0.18	0.27	0.27	0.18	0.18	0.52	0.52
19	0.22	0.33	0.16	0.12	0.13	0.33	0.16	0.03	0.03
20	0.04	0.11	0.15	0.21	0.20	0.11	0.15	0.14	0.14

$R_{n3,30}$ and $R_{n3,SRSS}$, it is observed that, even for SDOF systems, if the horizontal accelerograms are uncorrelated it does not necessarily imply that their corresponding effects will also be uncorrelated. Moreover, large values of the correlation coefficients do not imply a poor accuracy of the rules.

8. Accuracy of the combination rules for harmonic motion of the base

One of the main objectives of this paper is to study the accuracy of the combination rules for complex MDOF systems subjected to earthquake loading. However, it is helpful to study the accuracy of the rules for simpler systems, as equivalent SDOF systems, and simpler dynamics excitations, as harmonics excitations of the base. It may give additional insights regarding the accuracy of the rules for complex structural systems since it will allow to eliminate the influence of higher modes of vibration and of several frequencies of the earthquakes and to propose in advance the degree of correlation of the components.

The accuracy of the rules and the correlation coefficients of the effects of the horizontal components for the MDOF and *equivalent* SDOF systems subjected to a harmonic acceleration of the base are discussed in this section of the paper. The base acceleration in the *N-S* structural direction is given by

$$\mathbf{P_X(t) = P_0 \sin\omega t} \tag{5}$$

and that of the *E-W* direction by

$$\mathbf{P_Y(t) = P_0 \sin(\omega t + \phi)} \tag{6}$$

where P_0 and ω are the amplitude and the frequency of the harmonic acceleration which are assumed to be 200 mm/sec^2 and 20 rad/sec, respectively. ϕ is the phase angle between the orthogonal horizontal accelerations which defines the degree of correlation of the harmonic components. $\phi=0^0$ and 90^0 correspond to totally correlated and uncorrelated components, respectively. As for the case of earthquake loading and MDOF systems, elastic and inelastic structural behaviors are considered. Thus, P_X and P_Y are first applied as defined above and then they are scaled up to produce significantly yielding in the models.

The accuracy of the rules for MDOF systems is first discussed. Each acceleration is applied separately first (Load Cases 15 and 16) and then the simultaneous action of both accelerations (Load cases 13 and 14). After that, the accuracies of the rules are estimated. The R_{30} and R_{SRSS} parameters are used for this purpose. They are essentially the same as $R_{n3,30}$ and $R_{n3,SRSS,}$ but now harmonic loading are used in the horizontal directions instead. The results are not shown. The major observations, however, are that the 30% and SRSS rules may underestimate or overestimate the combined elastic axial load for highly correlated components and that for totally uncorrelated components, the rules accurately estimate the elastic axial load. However, for inelastic behavior, the rules may underestimate or overestimate the combined axial load even for high values of the phase angle. The combined interstory shear is reasonably estimated practically in all the cases.

The accuracy of the rules and the correlation coefficients of the effects of the horizontal components for the *equivalent* SDOF systems are now discussed. The results for axial loads on the columns of Model 1E are presented in Figs. 6(a) through 6(d) for the 30% and SRSS rules. It must be noted that the values of R_{30} and R_{SRSS} are estimated for increments of ϕ of 18^o. The plots indicate, in general, that if $\phi \leq 72^0$, both rules may underestimate (columns NW and SE in Fig. 2) or overestimate (columns NE and SW) the combined response for elastic behavior (Figs. 6(a) and 6(c)); the level of underestimation or overestimation monotonically increases as the values of the phase angle decrease (increasing correlation). However, the rules reasonably estimate the combined axial load for all the columns when the phase angle is between 72^o and 90^o, it is when the correlation of the horizontal accelerations is relatively small. Unlike the case of elastic behavior, the values of R_{30} and R_{SRSS} for inelastic behavior don't monotonically tend to unity as ϕ varies from 0 to 90^0. Even for uncorrelated components there is an important level of underestimation (up to 30%). Plots for base shear were also developed but are not shown. It is shown that for elastic behavior both rules reasonable overestimate the combined base shear for all values of ϕ. For the case of inelastic behavior the base shear is also overestimated, the level of overestimation is smaller than that of elastic behavior, particularly for small values of ϕ. Plots for the R_{30} and R_{SRSS}, parameters, for axial load and base shear, are also estimated for Model 2E but the results are not showed. The main observations made for Model 1E also apply to Model 2E.

The correlation coefficients of the horizontal harmonic accelerations and those of their

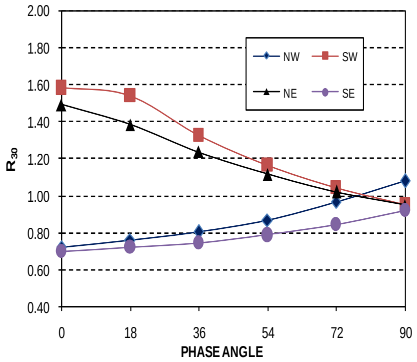

(a) R_{30} parameter, elastic behavior

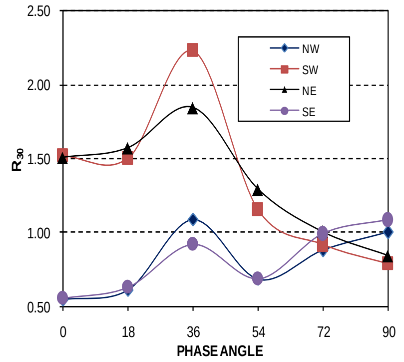

(b) R_{30} parameter, inelastic behavior

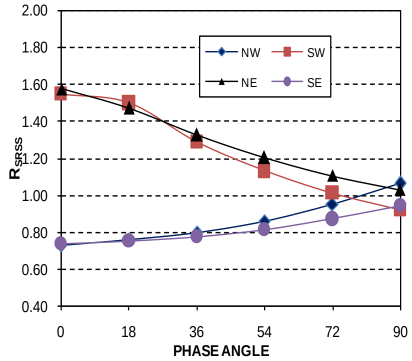

(c) R_{SRSS} parameter, elastic behavior

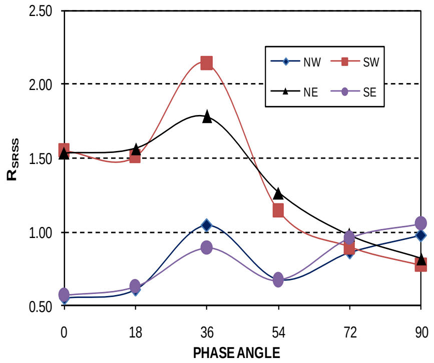

(d) R_{SRSS} parameter, inelastic behavior

Fig. 6 Accuracy of the rules for SDOF systems and harmonic loading, Model 1E

Table 11 Correlation coefficients (**ρ**) of the effect of individual components, SDOF systems and harmonic loading

MODEL (1)	Ø (2)	ρ_{HAR} (3)	ELASTIC AXIAL NW (4)	ELASTIC AXIAL SW (5)	ELASTIC AXIAL NE (6)	ELASTIC AXIAL SE (7)	ELASTIC SHEAR (8)	INELASTIC AXIAL NW (9)	INELASTIC AXIAL SW (10)	INELASTIC AXIAL NE (11)	INELASTIC AXIAL SE (12)	INELASTIC SHEAR (13)
1E	0°	1.00	1.00	1.00	1.00	1.00	1.00	1.00	1.00	1.00	1.00	1.00
	18°	0.95	0.95	0.94	0.94	0.95	0.34	0.95	0.95	0.95	0.95	0.40
	36°	0.81	0.79	0.79	0.79	0.79	-0.02	0.74	0.74	0.74	0.74	0.06
	54°	0.59	0.56	0.56	0.57	0.57	-0.04	0.56	0.56	0.56	0.56	0.02
	72°	0.31	0.29	0.29	0.30	0.29	-0.02	0.27	0.27	0.28	0.28	0.01
	90°	0.00	0.00	0.00	0.00	0.00	0.01	0.01	0.01	0.01	0.01	0.01
2E	0°	1.00	1.00	1.00	1.00	1.00	1.00	1.00	0.99	0.99	1.00	1.00
	18°	0.95	0.79	0.79	0.80	0.81	-0.14	0.79	0.79	0.82	0.82	-0.20
	36°	0.81	0.50	0.50	0.55	0.56	-0.12	0.50	0.50	0.57	0.57	-0.15
	54°	0.59	0.29	0.29	0.35	0.36	-0.08	0.29	0.30	0.37	0.37	-0.03
	72°	0.31	0.14	0.14	0.19	0.20	-0.04	0.16	0.16	0.22	0.21	-0.02
	90°	0.00	0.02	0.01	0.06	0.07	-0.01	0.05	0.05	0.08	0.06	0.00

individual effects, for shear and axial load, are given in Table 11. The ρ_{HAR} parameter represents the correlation of the harmonic components which are obviously the same for both models. As expected, for this simple loading and structural system, the correlations of the individual effects decrease as the correlation of the horizontal harmonic excitation decreases. From the results of Table 11 and Fig. 6, it is observed that small values of ρ implies a low correlation of the components but it is not necessarily associated to an accurate estimation of the combined response, particularly for inelastic behavior. Only for perfectly uncorrelated harmonic excitations and elastic analysis of SDOF systems, the individual effects of the components are uncorrelated and the rules accurately estimate the combined response. Whether the seismic response is underestimated or overestimated will depend, not only on the degree of correlation of the components, but also on the level of structural deformation, the type of response parameter, and the location of the particular structural member under consideration.

9. Conclusions

The Maximum seismic responses of steel buildings with perimeter moment resisting frames (MRF), modeled as complex multi-degree of freedom systems (MDOF), are estimated for several incidence angles of the horizontal components and the critical one is identified. The accuracy of the existing rules to combine of the individual effects of the seismic components, as well as the influence of the correlation of the components and the correlation of the effects on the accuracy of the rules, are considered. Some structural models considered in the SAC steel project are used in the study. The accuracy of the rules is also estimated for equivalent SDOF systems. Two and three components are considered. Results indicate that the critical response does not occur for principal components and that the corresponding incidence angle of the seismic components varies from one earthquake to another. In the general case, the critical response can be estimated as 1.40 and 1.10 times that of the principal components, for axial load and interstory shears, respectively, for the structural system under consideration. It is also observed that the rules underestimate the axial load but they reasonably overestimate the interstory and base shear. The uncertainty in the estimation is much larger for axial load than for shear, and, for axial load, it is much larger for inelastic than for elastic behavior. The effects of individual components may be highly correlated, not only for normal components, but also for totally uncorrelated components. Moreover, the rules are not always inaccurate in the estimation of the combined response for correlated components. On the other hand, totally uncorrelated components are not always related to an accurate estimation of the combined response. Only for perfectly uncorrelated harmonic excitations and elastic analysis of SDOF systems, the individual effects of the components are uncorrelated and the rules accurately estimate the combined response. In the general case, the level of underestimation or overestimation depends on the degree of correlation of the components, the type of structural system, the response parameter, the location of the structural member, and the level of structural deformation.

Acknowledgements

This paper is based on work supported by El Consejo Nacional de Ciencia y Tecnología (CONACyT) under grant 50298-J and by La Universidad Autónoma de Sinaloa (UAS) under grant PROFAPI-2012/148. Any opinions, findings, conclusions, or recommendations expressed in this

publication are those of the authors and do not necessarily reflect the views of the sponsors.

References

Beyer, K. and Bommer J.J. (2007), "Selection and scaling of real accelerograms for bi-directional loading: a review of current practice and code provisions", *J. Earthq. Eng*., **11**(1), 13-45.

Bisadi, V. and Head, M. (2010), "Orthogonal effects in nonlinear analysis of bridges subjected to multicomponent earthquake excitation", *Proceedings of the ASCE 2010 Structures Congress.*

Bisadi, V. and Head, M. (2011), "Evaluation of Combination Rules for Orthogonal Seismic Demands in Nonlinear Time History Analysis of Bridges", *J. Bridge Eng.*, **16**(6), 711-717.

Bojorquez, E., Reyes-Salazar A., Terán-Gilmore A. and Ruiz, S.E. (2010), "Energy-based damage index for steel structures", *Steel Compos. Struct.*, **10**(4), 331-348.

Building Officials & Code Administration International (2003), 12th Edition, National Building Code.

Clough, R.W. and Penzien, J. (1993), *Dynamics of Structures*, Second Edition, McGraHill.

Gao, L. and Haldar, A. (1995), "Nonlinear seismic response of space structures with PR connections", *Int. J. Microcomput. Civ. Eng.*, **10**, 27-37.

Grant, D. (2011), "Response spectral matching of two horizontal ground-motion components", *J. Struct. Eng.*, **137**(3), 289-297.

Der Kiureghian, A. (1981), "A response spectrum method for random vibration analysis of MDOF systems", *Earthq. Eng. Struct. Dyn.*, **9**(5), 419-435.

Federal Emergency Management Agency (2000), *State of the Art Report on Systems Performance of Steel Moment Frames Subjected to Earthquake Ground Shaking*, SAC Steel Project, Report FEMA 355C.

Hernández, J.J. and López, O.A. (2003), "Evaluation of combination rules for peak response calculation in three-component seismic analysis", *Earthq. Eng. Struct. Dyn.*, **32**(10), 1585-1602.

International Code Council (2003), *International Building Code (IBC)*, Falls Church, VA.

Lopez, O.A., Chopra, A.K. and Hernandez, J.J. (2000) "Critical response of structures to multi-component earthquake excitation", *Earthq. Eng. Struct. Dyn.*, **29**(12), 1759-1778.

Lopez, O.A. and Torres, R. (1995), "A clarification of orthogonal effects in a three-dimensional seismic analysis", *Earthq. Spectra*, **11**(4), 659-666.

Lopez, O.A., Chopra, A.K and Hernandez, J.J. (2004), "Adapting the CQC3 rule for three seismic components with different spectra", *J. Struct. Eng*., ASCE, **130**(3), 403-410.

Lopez, O.A., Chopra, A.K and Hernandez, J.J. (2001), "Evaluation of combination rules for maximum response calculation in multi-component seismic analysis", *Earthq. Eng. Struct. Dyn.*, **30**(9), 1379-1398.

Lopez, O.A, Hernandez J.J., Bonilla, R. and Fernandez A. (2006), "Response spectra for multi-component structural analysis", *Earthq. Spectra*, **22**(1), 85-113.

Mackie, K.R. and Cronin K.J. (2011), "Response sensitivity of highways bridges to randomly oriented multi-component earthquake excitation", *J. Earthq. Eng.*, **15**(6), 850-876.

Menun, C. and Der Kiureghian, A. (2000), "Envelopes for seismic response vectors. I: Theory", *J. Struct. Eng.*, ASCE, **126**(4), 467-473.

Menun, C. and Der Kiureghian, A. (1998), "A replacement for the 30%, 40% and SRSS rules for multi-component seismic analysis", *Earthq. Spectra*, **14**(1), 153-156.

Newmark, N.M. (1975) "Seismic design criteria for structures and facilities, Trans-Alaska pipeline system", *Proceedings of the U.S. National Conference on Earthquake Engineering.*

Newmark, N.M. and Hall, W.J. (1982), *Earthquake Spectra and Design*, Monograph Series, Earthquake Engineering Institute, Berkeley CA, USA.

Penzien, J. and Watabe, M. (1975), "Characteristics of 3-Dimensional earthquake ground motions", *Earthq. Eng. Struct. Dyn*., **3**(4), 365-373.

Reglamento de construcciones del Distrito Federal (2004), Normas Técnicas Complementarias de Diseño por Sismo, *Gaceta Oficial del Distrito Federal*, México City.

Reyes-Salazar, A., Haldar, A. and Romero-Lopez, M.R. (2000), “Force reduction factor for SDOF and MDOF”, *Joint Specialty Conference on Probabilistic Mechanics and Structural*, ASCE, Paper 063.

Reyes-Salazar, A. (1997), “Inelastic seismic response and ductility evaluation of steel frames with fully, partially restrained and composite connections”, Ph.D. thesis, Department of Civil Engineering and Engineering Mechanics, University of Arizona, Tucson, Arizona.

Reyes-Salazar, A. and Haldar, A. (1999), “Nonlinear seismic response of steel structures with semi-rigid and composite connections”, *J. Constr. Steel Res.*, **51**(1), 37-59.

Reyes-Salazar, A. and Haldar, A. (2000), “Dissipation of energy in steel frames with PR connections”, *Struct. Eng. Mech.*, **9**(3), 241-256.

Reyes-Salazar, A. and Haldar, A. (2001a), “Energy dissipation at PR frames under seismic loading”, *J. Struct. Eng*., ASCE, **127**(5), 588-593.

Reyes-Salazar, A. and Haldar, A. (2001b), “Seismic response and energy dissipation in partially restrained and fully restrained steel frames: An analytical study”, *Steel Compos. Struct*., **1**(4), 459-480.

Reyes-Salazar, A., Juarez-Duarte, J.A., López-Barraza, A. and Velázquez-Dimas, J.I. (2004), “Combined effect of the horizontal components of earthquakes for moment resisting steel frames”, *Steel Compos. Struct*., **4**(3), 89-209.

Reyes-Salazar, A., López-Barraza, A., López-López, L.A. and Haldar, A. (2008), “Multiple-components seismic response analysis-A critical review”, *J. Earthq. Eng*., **12**(5), 779-799.

Rigato, A.B. and Medina, R.A. (2007), “Influence of angle of incidence on seismic demands for inelastic single-storey structures subjected to bi-directional ground motions”, *Eng. Struct*., **29**(10), 2593-2601.

Rosenblueth, E. (1980), *Design of Earthquake Resistance Structures*, Pentech Press Ltd.

Rosenblueth, E. and Contreras, H. (1977), “Approximate design for multi-component Earthquakes”, *J. Eng. Mech. Div*., ASCE, **103**(5), 895-911.

Salmon, C.G., Johnson, J.E. and Malhas, F.A. (2009), *Steel Structures Design and Behavior*, Fifth Edition, Pearson, Prentice Hall, New Jersey.

Smeby, W. and DerKiureghian, A. (1985), “Modal combination rules for multi-component earthquake excitation”, *Earthq. Eng. Struct. Dyn.*, **13**(1), 1-12.

Shi, G. and Atluri, S.N. (1988), “Elasto-plastic large deformation analysis of spaces-frames”, *Int. J. Numer. Meth. Eng*., **26**(3), 589-615.

Tsourekas, A. and Athanatopoulou, A. (2013), “Evaluation of existing combination rules for the effects caused by three spatial components of an Earthquakes”, *KSCE J. Civ. Eng*., **17**(7),1728-1739.

Uniform Building Code (1994), *Structural Engineering Design Provisions Vol. 2*, International Conference of Building Officials.

Wilson, E.L., Suharwardy, I. and Habibullah, A. (1995), “A Clarification of the orthogonal effects in a three-dimensional seismic analysis”, *Earthq. Spectra*, **11**(4), 659-666.

Wilson, E.L., Der Kiureghian, A. and Bayo, E.P. (1981), “A replacement for the SRSS method in seismic analysis”, *Earthq. Eng. Struct. Dyn.*, **9**(2), 187-194.

CC